Genetic Deletion of the Adenosine A_{2A} Receptor Confers Postnatal Development of Relative Myopia in Mice

Xiangtian Zhou,[1,2,3,4] *Qinzhu Huang,*[1,2,3,4] *Jianhong An,*[1,2,3,4] *Runxia Lu,*[1,2,3,4] *Xiaoyi Qin,*[1,2,3,4] *Liqin Jiang,*[1,2,3,4] *Yuan Li,*[1,2,3,4] *Jianhua Wang,*[5] *Jiangfan Chen,*[*,6] *and Jia Qu*[*,1,2,3,4]

Purpose. To critically evaluate whether the adenosine A_{2A} receptor ($A_{2A}R$) plays a role in postnatal refractive development in mice.

Methods. Custom-built biometric systems specifically designed for mice were used to assess the development of relative myopia by examining refraction and biometrics in $A_{2A}R$ knockout (KO) mice and wild-type (WT) littermates between postnatal days (P)28 and P56. Ocular dimensions were measured by customized optical coherence tomography (OCT), refractive state by eccentric infrared photorefraction (EIR), and corneal radius of curvature by modified keratometry. Scleral collagen diameter and density were examined by electron microscopy on P35. The effect of $A_{2A}R$ activation on collagen mRNA expression and on soluble collagen production was examined in cultured human scleral fibroblasts by real-time RT-PCR and a collagen assay kit.

Results. Compared with WT littermates, the $A_{2A}R$ KO mice displayed relative myopia (average difference, 5.1 D between P28 and P35) and associated increases in VC depth and axial length from P28 to P56. Furthermore, the myopic shift in $A_{2A}R$ KO mice was associated with ultrastructural changes in the sclera: Electron microscopy revealed denser collagen fibrils with reduced diameter in $A_{2A}R$ KO compared with WT. Last, $A_{2A}R$ activation induced expression of mRNAs for collagens I, III, and V and increased production of soluble collagen in cultured human scleral fibroblasts.

Conclusions. Genetic deletion of the $A_{2A}R$ promotes development of relative myopia with increased axial length and altered scleral collagen fiber structure during postnatal development in mice. Thus, the $A_{2A}R$ may be important in normal refractive development. (*Invest Ophthalmol Vis Sci.* 2010;51:4362–4370) DOI:10.1167/iovs.09-3998

Myopia, the most common refractive defect in humans, is increasing significantly in prevalence and severity in many parts of the world.[1–3] Although low degrees of myopia cause impaired visual acuity that can be addressed with corrective lenses, higher degrees of myopia can lead to permanent visual impairment or blindness and can increase susceptibility to a range of ocular complications, such as glaucoma, retinal degeneration, and choroidal neovascularization.[4–7] Although the precise mechanism underlying the developmental regulation of myopia remains to be determined, various neuromodulators and hormone factors, including TGF-β,[8–10] dopamine,[11] and retinoic acid,[12] have been shown to play central roles in myopia and vision development. Development of myopia is at least partially attributable to excessive increases in axial length and marked changes in the sclera.[13] Scleral thinning and tissue loss occur rapidly during myopia's development.[14] In animal models of myopia, sclera thinning is associated with net loss of matrix, smaller diameter collagen fibrils in the sclera, and reduced collagen production.[14–17]

We hypothesized that the adenosine A_{2A} receptor ($A_{2A}R$) plays an important role in postnatal refractive development in mice by controlling collagen synthesis in scleral fibroblasts. The extracellular adenosine level in mammalian retina is regulated by light/dark conditions,[18] an important component of the visual signal that contributes to eye growth control and possibly to development of myopia.[19–22] A_{2A}Rs are expressed in ocular tissue, including in the ciliary processes, retina, retinal pigment epithelium, choriocapillaris, and scleral fibroblasts.[23,24] Of interest, $A_{2A}R$ activity can modulate collagen synthesis and extracellular matrix production in various cell types and tissues. For example, the $A_{2A}R$ agonist CGS21680 dose dependently increases collagen production in cultured human hepatic stellate cells[25] and promotes tissue repair, wound healing, and matrix production in skin in vivo.[26,27] Conversely, genetic deletion or pharmacologic blockade of A_{2A}Rs attenuates the fibrogenic process in liver[28] and skin.[29] Together, these studies raise the interesting possibility that $A_{2A}R$ activity influences the development of myopia by modulating collagen synthesis in the sclera.

In this study, we used $A_{2A}R$ KO mice and custom-built biometric systems specifically designed for mice to critically evaluate the role of $A_{2A}R$ in development of relative myopia at refractive and biometric levels, and we used electron microscopy to examine the ultrastructure. We detected a greater myopic shift, increased vitreous chamber depth and axial

From the [1]School of Optometry and Ophthalmology and Eye Hospital, Wenzhou Medical College, Wenzhou, China; the [2]State Key Laboratory Cultivation Base and [3]Key Laboratory of Vision Science, Ministry of Health, and the [4]Zhejiang Provincial Key Laboratory of Ophthalmology and Optometry, Zhejiang, China; [5]Bascom Palmer Eye Institute, Miller School of Medicine, University of Miami, Miami, Florida; and the [6]Department of Neurology, Boston University School of Medicine, Boston, Massachusetts.

Supported by National Natural Science Foundation of China Grants 30500549, 30600174, and 30830107; Zhejiang Provincial Natural Science Foundation of China Grants R205739 and Z205735; Zhejiang Provincial Program for the Cultivation of High-level Innovative Health Talents; and U.S. Public Health Service Grant NIH R01 NS048995.

Submitted for publication May 18, 2009; revised August 27 and December 13, 2009, and January 27 and February 17, 2010; accepted March 26, 2010.

Disclosure: **X. Zhou**, None; **Q. Huang**, None; **J. An**, None; **R. Lu**, None; **X. Qin**, None; **L. Jiang**, None; **Y. Li**, None; **J. Wang**, None; **J. Chen**, None; **J. Qu**, None

*Each of the following is a corresponding author: Jia Qu, School of Ophthalmology and Optometry, Wenzhou Medical College, 270 Xueyuan Road, Wenzhou, Zhejiang, China, 325027; jqu@wz.zj.cn.
Jiangfan Chen, Department of Neurology, Boston University School of Medicine, Boston, MA 02118; chenjf@bu.edu.

Investigative Ophthalmology & Visual Science, September 2010, Vol. 51, No. 9

length, and reduced scleral collagen fibril diameters in $A_{2A}R$ KO mice than in their wild-type littermates. In addition, we found that $A_{2A}R$ activation increases expression of mRNAs for collagens I, III, and V and soluble collagen production in cultured human fibroblasts. Together, these results provide the first evidence that the $A_{2A}R$ plays a role in controlling postnatal development of myopia in mice.

Materials and Methods

Animals

The treatment and care of animals was conducted according to the ARVO Statement for the Use of Animals in Ophthalmic and Vision Research, and the protocol for handling animals was approved by the Animal Care and Ethics Committee at Wenzhou Medical College (Wenzhou, China). $A_{2A}R$ KO mice were generated by Chen et al.,[30] originally in the mixed C57BL/6 background and more recently in a congenic C57BL/6 background which significantly reduces the potential confounding effect of genetic background.[31,32] In this study, heterozygous female mice were mated with heterozygous males so that both $A_{2A}R$ KO and WT littermates were generated from the same breeding pairs. The genotypes of the mice were determined by PCR analysis of tail DNA, as described previously.[31,32]

Biometric Measurements

Biometric measurements, including corneal radius of curvature, refractive state, and ocular dimensions, were taken once per week from postnatal day (P)28 to P56. These measurements were performed by a research optometrist who was blind to the genotypes of the mice.

Keratometry. Corneal curvature was measured with a keratometer (OM-4; Topcon, Tokyo, Japan) which was modified by mounting a +20.0-D aspherical lens. A group of stainless-steel ball bearings with diameters ranging from 2.0 to 3.98 mm were used for calibration. The corneal radius of curvature measured in the mice was then deduced from the readings on the balls with known radii.[33] Each eye was measured three times to obtain a mean value.

Refraction and Pupil Size. Refractive state and pupil size were measured in a darkened room with an eccentric infrared photorefractor (EIR).[33,34] Briefly, the mouse was gently restrained by grabbing its tail and positioning it on a small stage in front of the photoretinoscope. The position of the stage was swiftly adjusted until a clear first Purkinje image was seen in the center of the pupil, meaning an on-axis measurement. The data were then recorded by using software designed by Schaeffel et al.[34] Measurements were repeated at least three times for each eye.

Ocular Dimensions. Ocular dimensions, including anterior chamber (AC) depth, lens thickness, vitreous chamber (VC) depth, and axial length (AL), were measured by real-time optical coherence tomography (a custom-built OCT).[35] AC depth was defined as the distance from the posterior surface of the cornea to the anterior surface of the lens. AL was defined as the distance between the anterior surface of the cornea and the vitreous–retina interface. The configuration of the OCT was described in detail elsewhere,[36] as were the principle and the measurement process.[35] After being anesthetized, each mouse was placed in a cylindrical holder mounted on a positioning stage in front of the optical scanning probe. A video viewing system for observing the eye was used to monitor orientation and positioning. In addition, the optical axis of the mouse eye was aligned with the axis of the probe by detecting the specular reflex on the corneal apex and on the back apex of the lens in two-dimensional OCT images. Ocular dimensions were determined by moving the focal plane with the stepper motor and recording the distance traveled between two ocular interfaces. The recorded optical path length was then converted into a geometric path length by using the appropriate refractive indexes for each component of the eye. Each eye was scanned three times.

Electron Microscope

Mice were killed by an overdose of pentobarbitone sodium at P35. Three mice from each genotype group were evaluated. The anterior segment of the eye (including the cornea, iris, and crystalline lens) was cut away from the anterior scleral rim, and the vitreous body and retina were also dissected and discarded, leaving only the sclera. A 1.5-mm diameter trephine was used to punch out a tissue button from the sclera adjacent to the temporal margin of the optic disc.[16] The tissue button was immediately fixed in 2.5% glutaraldehyde with phosphate buffer (pH 7.4) for approximately 72 hours. The scleral tissue was processed further and sectioned for electron microscopic examination, as described elsewhere.[37] For transmission electron microscopy (model 7650; Hitachi, Tokyo, Japan), the scleral tissue button was equally divided into outer, middle, and inner layers (from the episclera), and five to six electron micrographs were taken from the middle layer of the sclera for each eye at ×30,000.

Analysis of fibril diameter and density was performed by a technician who was blind to the genotype. The diameter of fibrils was measured with image analysis software (Photoshop 10.0; Adobe Systems, San Jose, CA). Micrographs from nonoverlapping regions of the central portion of the sclera were taken from cross sections at ×30,000. For statistical analysis of fibril diameters, we adapted the method described by Ezura et al.[38] and Chakravarti et al.[39] in which the median of 100 to 300 diameter measurements from each micrograph was calculated and treated as one sample (WT: $n = 14$ micrographs, KO: $n = 20$ micrographs). Since the normality assumption was supported by the data ($P > 0.05$, K-S test), parametric methods were used in this analysis. To eliminate the difference in fibril number that may have affected histogram shape, we applied a percentage frequency histogram in the analysis (WT: $n = 1220$, KO: $n = 1897$).

The mean density of the scleral fibrils was estimated by determining the number of fibril cross sections from a randomly selected area (0.4 μm^2) in each micrograph. Fibrils showing only partial cross sections at boundaries of a counting area were excluded from analysis.

Cell Biology

Chemical Preparation. CGS21680 was first dissolved with DMSO to a concentration of 10 mM and then serially diluted with FBS-free DMEM, to obtain different concentrations. SCH58261 was dissolved in DMSO to a concentration of 1 mM, which was then diluted with FBS-free DMEM to 1 μM. Dissolving and diluting were performed in the darkroom under red lights.

Cell Culture. Normal human scleral fibroblasts (HSFs) were isolated from donor eyeballs.[40,41] The donor eyes were obtained and managed in accordance with the guidelines in the Declaration of Helsinki for research involving human tissue. The HSFs were maintained in DMEM supplemented with 10% fetal bovine serum, 100 U/mL penicillin, and 100 U/mL streptomycin. For treatment, culture medium was replaced by serum-free DMEM, and the cells were treated for 24 hours with or without CGS21680 (1 nM to 1 μM). For the group treated with both CGS21680 (1 μM) and SCH58261 (1 μM), the cells were incubated with 1 μM SCH58261 for 15 minutes before addition of CGS21680. After treatment, the medium was harvested, and total soluble collagen concentration was determined by collagen assay (Sircol; Biocolor, Ltd., Carrickfergus, UK). The cells were harvested for determination of collagen mRNA expression.

Immunohistochemistry of $A_{2A}Rs$ in HSFs. Untreated HSFs were used for immunohistochemistry of $A_{2A}Rs$. The primary antibody was a monoclonal mouse anti-$A_{2A}R$ (1:400; Upstate Biotechnology, Lake Placid, NY) ,and the secondary antibody was Cy3-conjugated goat anti-mouse (1:1500; Jackson Immunochemicals, West Grove, PA). Fluorescent images were then captured (AxioVision software; Carl Zeiss Meditec, Dublin, CA).

Real-Time RT-PCR. Total RNA was extracted from HSF cultures (Trizol reagent; Invitrogen-Gibco, Grand Island, NY) and 0.2 μg of RNA from each sample was reverse transcribed with M-MLV reverse tran-

TABLE 1. Sequences for Primers and RT-PCR Product Length

Gene	Forward Primer (5′–3′)	Reverse Primer (5′–3′)	Length (bp)
Collagen I	CGAGCGTGGTGTGCAAGGTC	CTGCACCACGTTCACCAGGC	158 bp
Collagen III	ACTCAAGTCTGTTAATGGAC	TATTCTCCACTCTTGAGTTC	120 bp
Collagen V	CAATGGACCCCAAGGACCCA	TTTCTCCCGTGGGACCCTGA	173 bp
GAPDH	GCTCTCTGCTCCTCCTGTTC	GACTCCGACCTTCACCTTCC	100 bp

scriptase according to the manufacturer's instructions (Promega, Madison, WI). The primers were designed on computer (Primer Express 3.0 software; Applied Biosystems, Inc. [ABI], Foster City, CA), and the sequences and product length are provided in Table 1. PCRs were performed in a real-time PCR system (model 7500; ABI), with 2× SYBR green PCR master mix (ABI). The results were normalized to the housekeeping gene GAPDH.

Sircol Collagen Assay. The total soluble collagen concentration in the cell supernatants was measured with the collagen assay kit (Sircol; Biocolor, Ltd.).[25] In brief, a 200-μL aliquot of supernatant was added to 1 mL of the dye from the kit, mixed in a mechanical shaker at room temperature for 30 minutes, and centrifuged to precipitate the collagen-dye complex at the bottom of the tube. The pellet was dissolved in 0.5 M NaOH, to release the collagen-dye complex, and the concentration of collagen was determined by absorbance at 540 nm in a spectrophotometer.

Statistics

To determine significance in our comparisons of biometric measurements, we used commercial software (Prism 4; GraphPad, San Diego, CA) for two-way, repeated-measures ANOVA, with one factor, to determine the main effects (genotype and postnatal day) and their interaction. Differences between genotypes at specific postnatal days were analyzed by the Bonferroni post hoc test. For collagen fiber diameter, the difference between genotypes was analyzed by independent *t*-test. The data on collagen mRNA levels and soluble collagen production were analyzed by one-way ANOVA with post hoc Bonferroni tests.

RESULTS

Relative Myopia and Associated Increase in AL and VC Length from P28 to P56

Consistent with previous reports,[33,42] the WT mice developed hyperopia over the period between P28 and P56, with greatest hyperopia at P56 (4.5 ± 1.1 D, mean ± SE; Fig. 1a). $A_{2A}R$ KO mice also developed hyperopia during this period, with greatest levels at P56 (2.4 ± 1.6 D). $A_{2A}R$ KO mice were more myopic than were the WT mice (WT: $n = 18$, KO: $n = 13$, main effect: $F_{(1,135)} = 15.25$, $P < 0.001$; interaction: $F_{(4,135)} = 0.54$, $P = 0.709$, two-way ANOVA for repeated measurements). Between P28 and P35, the $A_{2A}R$ KO was an average of 5.1 D more myopic than were the WT littermates. Post hoc comparison revealed a significant difference between genotypes at P28 ($P < 0.05$, two-way ANOVA, followed by post hoc Bonferroni test).

To further characterize the ocular growth in $A_{2A}R$ KO mice, we used our custom-built biometric equipment, which was specifically designed for mice, to determine the AL and other biometric parameters. AL in both genotypes increased significantly from P28 to P56. The most rapid increase took place between P28 and P42, followed by a small but significant increase during the remaining time. The AL in $A_{2A}R$ KO mice was significantly longer than in WT littermates at P28 (Fig. 1c; two-way ANOVA for repeated measurements; main effect: $F_{(1,125)} = 20.94$, $P < 0.001$; interaction: $F_{(4,125)} = 0.432$, $P = 0.785$; post hoc Bonferroni test indicated a significant difference between WT and $A_{2A}R$ KO groups at postnatal day 28 ($P < 0.05$).

Among all AL components, only VC length declined during postnatal development. VC in both genotypes gradually decreased between P28 and P56. However, the VC was greater in the $A_{2A}R$ KO mice than in the WT group (two-way ANOVA for repeated measurements; main effect: $F_{(1,150)} = 63.83$, $P < 0.0001$; interaction: $F_{(4,150)} = 1.48$, $P = 0.211$). There were significant differences between the genotypes at P28 ($P < 0.001$, two-way ANOVA, followed by post hoc Bonferroni test), P42 ($P < 0.001$), P49 ($P < 0.05$), and P56 ($P < 0.01$; Fig. 1b, Table 2).

Normal Growth in the Anterior Segment in $A_{2A}R$ KO Mice

Corneal radius of curvature in both genotypes increased rapidly during postnatal development, but was not significantly different between the two genotypes (main effect: $F_{(1,30)} = 1.35$, $P = 0.25$, Fig. 2a). Corneal radius of curvature in $A_{2A}R$ KO mice increased from 1.37 ± 0.006 mm at P28 to 1.49 ± 0.005 mm at P56, comparable to the increase from 1.36 ± 0.008 to 1.48 ± 0.008 mm seen for WT littermates.

Similarly, AC depth in both genotypes increased during postnatal development. The AC in WT mice increased from

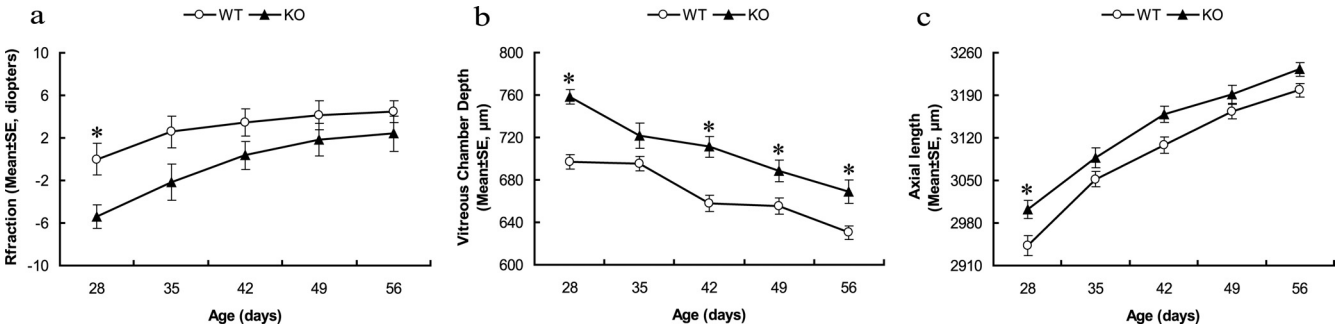

FIGURE 1. $A_{2A}R$ KO mice exhibited a greater myopic shift and greater VC depth and AL than in the WT littermates during postnatal development. Comparison of refractive status (**a**), VC depth (**b**), and AL (**c**) between $A_{2A}R$ KO mice and WT littermates at the indicated postnatal time points. *$P < 0.05$; two-way ANOVA for repeated measurements post hoc Bonferroni test, WT: $n = 18$, KO: $n = 13$.

309 ± 4 μm (mean ± SE) at P28 to 369 ± 3 μm at P56. AC in $A_{2A}R$ KO mice also increased from 299 ± 6 μm at P28 to 371 ± 6 μm at P56. There was no significant difference between the two genotypes (main effect: $F_{(1,150)} = 2.53$, $P = 0.114$, Fig. 2b). Lens thickness increased comparably in both genotypes during postnatal development (main effect: $F_{(1,150)} = 2.47$, $P = 0.118$, Fig. 2c). At P28, lens thickness (LT) in WT mice was 1544 ± 8 μm (mean ± SE), comparable to 1535 ± 8 μm (mean ± SE) in $A_{2A}R$ KO mice. At P56, LT was 1734 ± 7 μm in WT and 1722 ± 7 μm in $A_{2A}R$ KO.

To evaluate whether the development of myopia is confounded by pupil size or body weight in $A_{2A}R$ KO mice, we examined both during postnatal development. Pupil size increased in both genotypes with no significant difference between them (main effect: $F_{(1,145)} = 0.123$, $P = 0.727$, Fig. 2d). Similarly, body weight increased steadily in both genotypes during postnatal development (Table 2), comparable with results in a previous report,[43] with no significant difference between the two genotypes at any time point (main effect: $F_{(1,155)} = 2.650$, $P = 0.105$, Table 2).

Myopia Associated with Thinner but Denser Collagen Fibrils in the Posterior Sclera

To investigate the possible ultrastructural basis for the development of myopia in the absence of A_{2A}Rs, we evaluated the fibril diameter in sclera of $A_{2A}R$ KO mice and WT littermates at P35 by electron microscopy. Ultrastructural analysis revealed that the collagen fibrils from posterior scleral regions of WT mice had wider mean cross-sectional diameters than those in $A_{2A}R$ KO mice (Figs. 3a, 3c). Quantitative analysis showed that this difference in diameters was significant (WT: 69.78 ± 9.20 nm, KO: 59.32 ± 11.87 nm, $P = 0.009$, independent *t*-test; Figs. 3b, 3d). Consistent with the smaller diameter, the density of the scleral fibrils per square millimeter in $A_{2A}R$ KO mice (173.31 ± 42.26/mm^2) was significantly higher than in WT littermates (141.72 ± 34.19/mm^2; $P = 0.02$, independent *t*-test).

Effect of Activation of the $A_{2A}R$ on Expression of mRNAs for Collagens I, III, and V and Production of Total Soluble Collagen in Cultured HSFs

To further investigate the biochemical basis for reduced scleral fibril diameter, we examined the effect of adenosine agonists and antagonists on expression of the mRNAs for collagen I, III, and V and production of total soluble collagen in cultured HSFs. We focused our analysis on types I, III, and V because they are the major types found in sclera of human and other species[14] and development of myopia has been associated with reduction of type I collagen.[15,44] Furthermore, these collagens contribute to collagen fibril diameter during fibrillogenesis,[45] and they are regulated by $A_{2A}R$ activation in hepatic stellate cells.[25] Human fibroblasts were used due to the technical difficulty of establishing mouse scleral fibroblasts and because of the possible relevance to human myopia. We first confirmed the expression of A_{2A}Rs in cultured HSFs by indirect immunofluorescence. We detected strong $A_{2A}R$ expression in the cytosol and membrane of cultured HSFs, but not in the nucleus (Fig. 4a). No fluorescent signal was detected when anti-$A_{2A}R$ antibody was omitted from the reaction or when striatum from $A_{2A}R$ KO mice was probed with the same antibody (data not shown), indicating that the staining is specific.

We treated cultured HSFs with the $A_{2A}R$ agonist CGS21680 (1 nM to 1 μM) in the absence or presence of the $A_{2A}R$ antagonist SCH58261 (1 μM) for 24 hours. As shown in Figure 4b, CGS21680 increased levels of mRNAs for collagen I, III, and V in an apparently concentration-dependent manner. At 1 μM, CGS21680 significantly increased the level of collagen I, III, and V mRNAs compared with that in vehicle-treated cells ($P < 0.01$, one-way ANOVA, post hoc Bonferroni test). Conversely, SCH58261 (1 μM) significantly decreased collagen production. Furthermore, co-treatment with the $A_{2A}R$ antagonist SCH58261 also abrogated the effect of CGS21680 on collagen mRNA expression ($P < 0.01$, one-way ANOVA, post hoc Bonferroni test, CGS21680 [1 μM] vs. CGS21680 [1 μM] + SCH58261 [1 μM]).

To further explore regulation of collagen synthesis by $A_{2A}R$, we used a collagen assay kit (Sircol; Biocolor, Ltd.) to determine the effect of $A_{2A}R$ agonists and antagonists on total soluble collagen production in HSFs.[25] At 1 μM, the $A_{2A}R$ agonist CGS21680 significantly increased soluble collagen production in HSF compared with the vehicle-treated cells (Fig. 4c; $P = 0.04$, one-way ANOVA, post hoc Bonferroni test). After treatment with 1 μM SCH58261, collagen production decreased markedly to below the detection limit of the collagen assay (data not shown). Co-treatment with the $A_{2A}R$ antagonist SCH58261 abrogated the effect of CGS21680 on collagen production ($P < 0.01$, one-way ANOVA, post hoc Bonferroni tests, CGS21680 [1 μM] vs. CGS21680 [1 μM] + SCH58261 [1 μM]).

Table 2. Various Biometric Parameters Comparison between WT and KO Mice between Days 28 and 56

Age (d)	Group	Refraction (D)*	Pupil Size (mm)	AC Depth (μm)	Lens Thickness (μm)	VC Depth (μm)*	AL (μm)*	Body Weight (g)	Corneal Curvature (mm)
P28	WT	0.0 ± 1.5	2.18 ± 0.02	309 ± 4	1544 ± 8	697 ± 7	2943 ± 17	12.31 ± 0.58	1.37 ± 0.006
P28	KO	−5.4 ± 1.1†	2.17 ± 0.02	299 ± 6	1535 ± 8	758 ± 7†	3002 ± 14†	11.28 ± 0.69	1.36 ± 0.008
P35	WT	2.6 ± 1.5	2.28 ± 0.02	335 ± 4	1609 ± 6	695 ± 7	3052 ± 13	17.03 ± 0.47	1.42 ± 0.005
P35	KO	−2.2 ± 1.7	2.30 ± 0.02	334 ± 4	1606 ± 7	722 ± 12	3087 ± 16	16.54 ± 0.62	1.42 ± 0.007
P42	WT	3.4 ± 1.3	2.37 ± 0.02	353 ± 4	1667 ± 6	658 ± 7	3108 ± 14	19.20 ± 0.46	1.45 ± 0.005
P42	KO	0.3 ± 1.3	2.34 ± 0.02	343 ± 4	1659 ± 6	711 ± 10†	3158 ± 14	18.70 ± 0.51	1.43 ± 0.005
P49	WT	4.1 ± 1.4	2.36 ± 0.02	355 ± 4	1695 ± 8	655 ± 8	3164 ± 12	20.23 ± 0.54	1.47 ± 0.005
P49	KO	1.8 ± 1.5	2.36 ± 0.02	359 ± 3	1689 ± 7	688 ± 10†	3191 ± 16	19.33 ± 0.55	1.46 ± 0.008
P56	WT	4.5 ± 1.1	2.42 ± 0.01	369 ± 3	1734 ± 7	630 ± 6	3199 ± 11	22.12 ± 0.47	1.49 ± 0.005
P56	KO	2.4 ± 1.6	2.43 ± 0.01	371 ± 6	1722 ± 7	669 ± 11†	3233 ± 11	21.38 ± 0.64	1.48 ± 0.008

Data are expressed as the mean ± SE (WT: $n = 18$, KO: $n = 13$). Significance was determined by two-way ANOVA for repeated measurements for the main effects (genotype and postnatal day) and their interaction, followed by Bonferroni post hoc comparison to determine the difference between the genotypes at specific postnatal days.

* Significant main effect (i.e. genotype) by two-way ANOVA for repeated measurements. For refraction: $F_{(1,135)} = 15.24$, $P < 0.01$; for vitreous chamber depth: $F_{(1,150)} = 64.83$, $P < 0.01$; for axial length: $F_{(1,125)} = 20.94$, $P < 0.01$.

† Significant difference ($P < 0.05$) between the genotypes (Bonferroni post hoc comparisons).

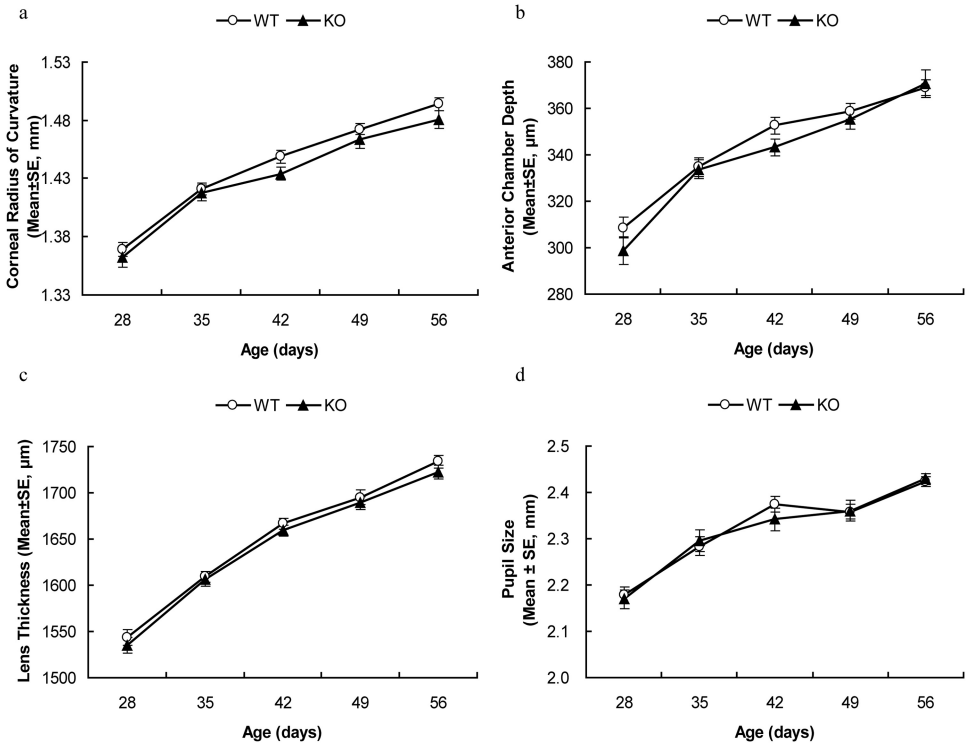

FIGURE 2. Postnatal development of corneal curvature, AC depth, lens thickness, and pupil size were indistinguishable between $A_{2A}R$ KO mice and WT littermates. $A_{2A}R$ KO mice and WT littermates were evaluated for corneal curvature (**a**), chamber depth (**b**), lens thickness (**c**), and pupil size (**d**) once a week from P28 to P56. There was no significant difference in any of these biometric measurements during this time period ($P > 0.05$, two-way ANOVA for repeated measurements).

DISCUSSION

Recently, three studies have shown that relative myopia can be induced in mice by targeted deletion of genes, including *Egr-1*, *Nyx*, and a double deletion of lumican and fibromodulin.[39,46,47] However, because of the technical limitations of biometric measurements in mice, refractive status,[39] and important biometric parameters of myopia, such as VC depth and crystalline lens thickness, were not evaluated in these studies.[46,47] Our custom-built OCT and the EIR designed by Schaeffel et al.[34]allowed us to overcome these limitations and more accurately measure refractive status and other important biometric parameters in mice.[33,35] Refractive error during postnatal development in mice progresses to more hyperopia, reaching a peak at P47 or P55 and then leveling off and remaining stable thereafter.[33,42] The WT mice in our present study displayed similar trends within the time frame of the study. Of note, $A_{2A}R$ KO mice were on average 5.1 D more myopic than were WT mice at P28 and P35. Detailed measurements of VC length, AC depth, and corneal curvature demonstrate that development of relative myopia in $A_{2A}R$ KO mice is associated with longer AL, particularly in the VC, but not with altered corneal curvature or AC depth. These biometric changes in $A_{2A}R$ KO mice closely resemble those seen in human myopia which features higher myopic diopters, longer VC depth and AL, but no change in corneal radius of curvature and lens thickness.[48–50] In contrast to the *Egr-1* mutant mice, where the result was complicated by the potential confounding effects of reduced body weight, indicating general growth impairment,[46] the effect we see in $A_{2A}R$ KO mice cannot be attributed to gross growth changes, since body weight is indistinguishable between $A_{2A}R$ KO mice

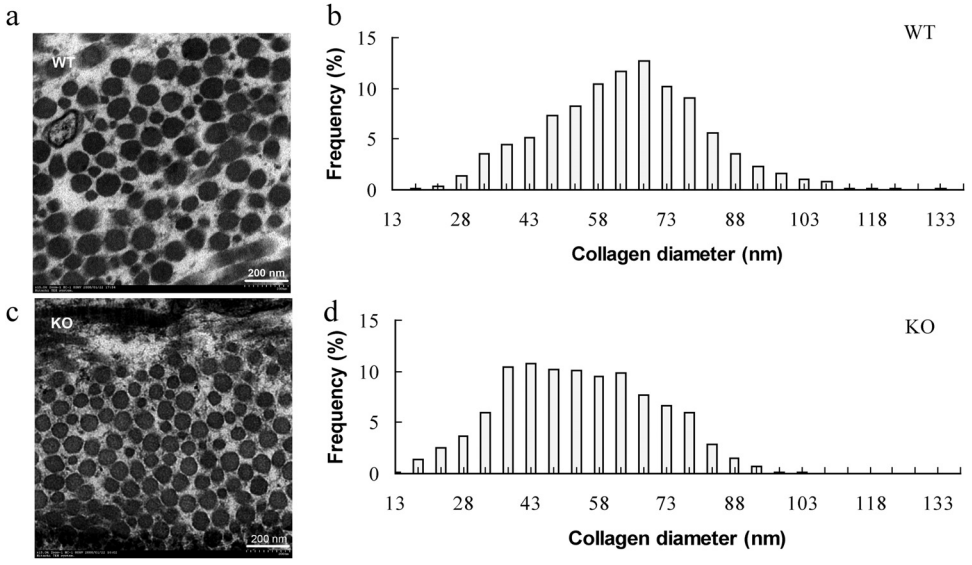

FIGURE 3. Ultrastructural analysis of collagen fibers in sclera of $A_{2A}R$ KO mice and WT littermates at P35. Collagen fibrils were examined by electron microscopy (EM), and fibril diameters were quantified in posterior sclera of $A_{2A}R$ KO and WT littermates at P35. Representative EM photographs show collagen fibrils in posterior sclera of $A_{2A}R$ KO mice (**c**) and WT littermates (**a**). Distribution histograms of fibril diameters in WT (**b**) and $A_{2A}R$ KO (**d**) mice at P35 reveal that collagen fibrils from posterior scleral regions of $A_{2A}R$ KO mice had significantly smaller mean cross-sectional diameters than that those of WT mice (WT: 69.78 ± 9.20 nm, KO: 59.32 ± 11.87 nm, $P < 0.01$, *t*-test).

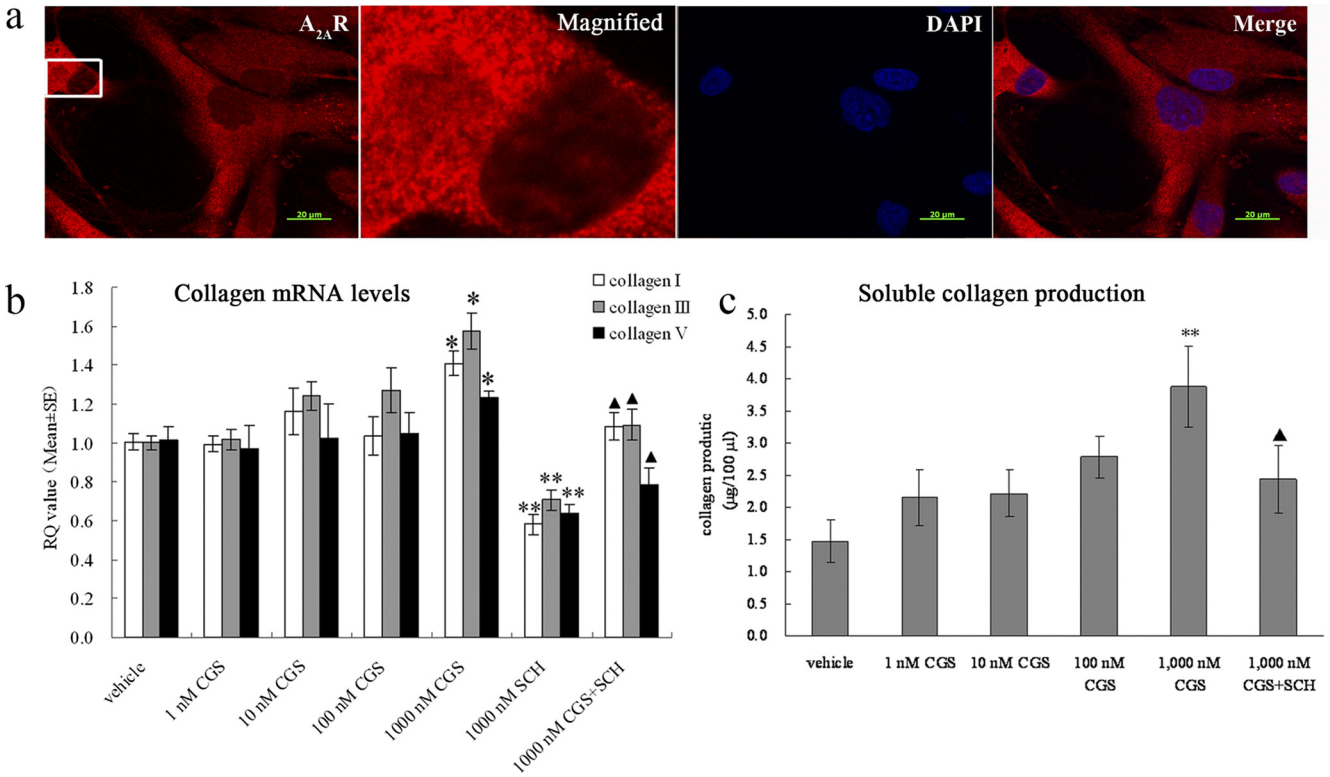

FIGURE 4. Activation of the $A_{2A}R$ increases the expression of mRNAs for collagen I, III, and V and the total soluble collagen production in cultured HSFs. (**a**) Immunofluorescent analysis of $A_{2A}R$ distribution in HSFs. Cultures were immunostained with antibody specific for $A_{2A}R$ and with DAPI, to visualize the nuclei. *Left* to *right*: anti-$A_{2A}R$ staining (*red*); 5× enlargement of the marked region; DAPI (*blue*) staining of the same enlarged region; and the merged image. Bar, 20 μm. (**b**) Collagen mRNA levels. HSFs were cultured and treated with different concentrations of CGS21680 and SCH58261. RQ (relative quantity) value is the mean change ratio in expression of the target gene. $^{*}P < 0.05$, CGS21680 versus vehicle. $^{**}P < 0.05$, SCH58261 versus vehicle. $\blacktriangle P < 0.01$, CGS21680 versus CGS21680 and SCH58261 ($n = 6$, one-way ANOVA, post hoc Bonferroni test). (**c**) Soluble collagen production. HSFs were cultured and treated with different concentrations of CGS21680 and SCH58261. $^{**}P < 0.05$, CGS21680 versus vehicle. $\blacktriangle P < 0.05$, CGS21680 versus CGS21680+SCH58261 ($n = 6$, one-way ANOVA, post hoc Bonferroni test).

and WT littermates. An earlier report stated that a 0.1-mm increase in pupil size could contribute to 0.8-D hyperopia when measured with EIR.[34] Our measurements showed that pupil size was not a factor in the difference we saw between $A_{2A}R$ KO and WT littermates. Furthermore, the normal development of corneal curvature, AC depth, and lens thickness strongly argue that the development of relative myopia in $A_{2A}R$ KO mice is not the result of any general difference in eye growth. The refractive shift in $A_{2A}R$ KO mice is also unlikely to be due to alterations in other organs and systems, because few physiological changes (with the exception of heart rate and metabolic rate[51] and basal locomotor activity[30,52]) have been described during postnatal development in naïve animals of this line of $A_{2A}R$ KO mice.[53] Most studies, including ours, have uncovered different phenotypes in these animals after pathologic insults or stress, or in response to particular pharmacologic treatments, consistent with an important pathophysiological role of the $A_{2A}R$.

The magnitude of the change in refractive status in $A_{2A}R$ KO animals was comparable to that in *Egr-1* KO mice. However, *Egr-1* knockout mice exhibited a persistent refractive change, but only a temporary change in AL, whereas $A_{2A}R$ KO mice displayed a transient refractive change but a persistent change in AL. It was speculated that additional changes in lens thickness, curvature, and power may account for the difference between refractive and AL changes in *Egr-1* KO mice.[46] Our finding that WT and $A_{2A}R$ KO mice have identical lens thickness suggests that this parameter is not responsible for the return to normal refractive status that we see in $A_{2A}R$ KO mice. It is possible that the retarded emmetropization process may in part account for the myopic shift observed in the $A_{2A}R$ KO mice. Studies of myopia induced by form deprivation or lens defocus are needed, to clarify whether the myopic phenotype in $A_{2A}R$ KO mice is specifically associated with visual signals.

According to the schematic mouse eye,[42,54] 1 D of change corresponds to only a 4- to 5-μm change in AL. However, we found that at P28, when there is significant refractive difference between $A_{2A}R$ KO and WT mice, the AL difference between the genotypes was 59 nm, significantly larger than the values predicted by the model, which predicts changes of 20 to 25 μm. The reason for this discrepancy is not clear. However, it should be noted that, to date, no published study has reported AL changes and refractive errors that agree with the predictions of the mouse model eye.[46,55–57] A possible explanation for this is that the mouse model eye was based on in vitro measurements,[42] whereas most of the published studies, including ours, present in vivo measurements. Consistent with this explanation, in two reports published by the same group, the AL reported in frozen sections[42] was larger than that measured in vivo in mice of the same age.[55]

Differences between $A_{2A}R$ KO mice and WT littermates in refraction and AL were apparent only in young animals. By P56, neither refraction nor AL in $A_{2A}R$ KO was significantly different from those in WT. There are several possible explanations for this transient effect. It may reflect developmental changes in $A_{2A}R$ expression. Although there is no information available on developmental expression of $A_{2A}R$ in eye, $A_{2A}R$ mRNA in the brain increases during the first 3 weeks of postnatal development and then declines slightly to adult levels.[58,59] Thus, it is possible that $A_{2A}R$ activity is at its highest level in the eye

around the third postnatal week, resulting in the refractive change seen around this particular postnatal stage. Another possibility is that $A_{2A}R$ activity exerts the same effect on refractive status throughout development, but other factors contribute in later development, counteracting or minimizing the effect of the $A_{2A}R$.

In contrast to the transient change in refractive status and AL, VC depth remained significantly greater in $A_{2A}R$ KO than WT littermates throughout postnatal development. This difference in duration of effect is consistent with our recent finding that in hyperopic-defocus–induced myopia in the guinea pig, the defocused eyes rapidly developed toward hyperopia after removal of the defocusing lens, whereas the VC length in the defocused eyes returned toward normal much more slowly.[60] Changes in lens curvature, index, and power[42] may compensate for the longer VC depth later in development, resulting in return to normal refraction without a change in VC depth.

Current understanding of refractive development suggests that the sclera plays a pivotal role in the control of eye size and the development of myopia.[61] Thus, our finding of longer AL, particularly in the VC, led us to investigate possible alterations in scleral structure in $A_{2A}R$ KO mice. The association we observed between postnatal development of relative myopia in $A_{2A}R$ KO mice and ultrastructural changes in collagen fibers in the sclera is consistent with previous studies. Studies in human myopia and in animal models of myopia have demonstrated that scleral thinning, tissue loss, and reduced collagen fibril diameter are associated with ocular enlargement and development of myopia.[14,16,62–64] Scleral thinning is greatest at the posterior pole of the eye. Consistent with this notion, Chakravarti et al.[39] found that mice with a double mutation of lumican and fibromodulin (important regulators of scleral fibril synthesis) show certain features of high myopia including increased AL, thin sclera, and retinal detachment. Our electron microscopic examination (which provides more sensitive measurements than the thickness and dry weight used in many previous studies) revealed that collagen fibril diameter is reduced and the density of collagen fibrils is increased in the sclera of $A_{2A}R$ KO mice. This finding is consistent with the reduced collagen fibril diameter observed in myopic tree shrews,[16] and highly myopic human eyes,[64,65] as well as with the finding of increased numbers of fibril bundles across the sclera thickness in myopic tree shrews.[16]

There is little information about changes in scleral collagen fibril density during postnatal development of myopia. In the fibromodulin–lumican double mutants just described, collagen fibrils with both abnormally large and abnormally small diameters are found in the sclera, whereas mice with fibromodulin mutation alone have only the abnormally small diameter collagen fibrils. However, refraction was not evaluated in these animals.[39] In one study of form deprivation in tree shrews, McBrien et al.[16] reported an increased number of small diameter collagen fibrils in the sclera after long-term form deprivation, which is consistent with findings in humans and is likely to contribute to the weakened biomechanical properties of the sclera that have previously been reported. This conclusion is in apparent agreement with our finding of increased density of collagen bundles in myopic $A_{2A}R$ KO mice.

Our ultrastructural finding in $A_{2A}R$ KO mice suggested a possible histologic basis for the development of relative myopia in these animals and prompted us to investigate $A_{2A}R$ modulation of collagen synthesis in cultured HSFs (Fig. 4a).[24] Consistent with the ultrastructural changes, treatment with the $A_{2A}R$ agonist CGS21680 dose dependently increased collagen I, III, and V production in HSF in vitro, an effect that was blocked by the selective $A_{2A}R$ antagonist SCH58261. This finding suggests that $A_{2A}R$ activity directly affects collagen synthesis in scleral fibroblasts.

The modulation of scleral collagen by the $A_{2A}R$ is also in agreement with results reported in human hepatic stellate cells and human dermal fibroblasts.[25,28,29,66] In contrast with our results, an early report showed that 7-methylxanthine (7-mx), a metabolite of the nonselective adenosine receptor antagonist caffeine, increases collagen concentration and the diameter of collagen fibrils in the posterior sclera in rabbit.[67] More recently, 7-mx also was shown to reduce axial eye elongation and myopia progression in both guinea pigs and patients (Cui D, et al. *IOVS* 2008;49:ARVO E-Abstract 1736).[68] However, it was not clear which adenosine receptor was responsible for the effects seen in those studies, since there are four receptor subtypes and 7-mx is nonselective. One explanation for the discrepancy between our study and the 7-mx studies is that different adenosine receptors exert different effects on eye development. The 7-mx may block several receptor subtypes in the sclera, whereas the $A_{2A}R$ KO affects only the $A_{2A}R$. Caffeine and its methylxanthine metabolites block both A_1R and $A_{2A}R$ with similar low affinities; thus, it is possible that the activity of A_1R receptors also modulates the development of myopia, possibly by antagonizing the $A_{2A}R$ effect, since A_1R is mainly coupled to G_i and inhibits adenylyl cyclase, whereas $A_{2A}R$ usually stimulates adenylyl cyclase through coupling to G_s proteins.[69] Another possibility is that the effects are species specific, as has been reported for other factors associated with myopia. For example, retinoic acid levels change in the opposite direction in the choroids of marmoset and chicken during induction of myopia.[70]

Our biometric, histologic, and biochemical findings suggest that activation of the $A_{2A}R$ is essential for normal growth of refraction, AL, and VC in mice during postnatal development, possibly through control of collagen synthesis in the sclera. Our findings raise the possibility that therapies targeting the $A_{2A}R$ can modify the development of myopia. In addition, these findings invite genetic studies of $A_{2A}R$ polymorphism and epidemiologic studies of human caffeine consumption as they relate to the development of myopia.

Acknowledgments

The authors thank Frank Schaeffel for providing support on our eccentric infrared photorefractor.

References

1. Morgan I, Rose K. How genetic is school myopia? *Prog Retin Eye Res.* 2005;24:1–38.
2. Lin LL, Shih YF, Hsiao CK, Chen CJ. Prevalence of myopia in Taiwanese schoolchildren: 1983 to 2000. *Ann Acad Med Singapore.* 2004;33:27–33.
3. Lam CS, Goldschmidt E, Edwards MH. Prevalence of myopia in local and international schools in Hong Kong. *Optom Vis Sci.* 2004;81:317–322.
4. Wu SY, Nemesure B, Leske MC. Refractive errors in a black adult population: the Barbados Eye Study. *Invest Ophthalmol Vis Sci.* 1999;40:2179–2184.
5. Saw SM, Gazzard G, Shih-Yen EC, Chua WH. Myopia and associated pathological complications. *Ophthalmic Physiol Opt.* 2005;25:381–391.
6. Cohen SY, Laroche A, Leguen Y, Soubrane G, Coscas GJ. Etiology of choroidal neovascularization in young patients. *Ophthalmology.* 1996;103:1241–1244.
7. Blohme J, Tornqvist K. Visual impairment in Swedish children. III. Diagnoses. *Acta Ophthalmol Scand.* 1997;75:681–687.
8. McBrien NA, Jobling AI, Gentle A. Biomechanics of the sclera in myopia: extracellular and cellular factors. *Optom Vis Sci.* 2009;86:E23–E30.

9. Jobling AI, Wan R, Gentle A, Bui BV, McBrien NA. Retinal and choroidal TGF-beta in the tree shrew model of myopia: isoform expression, activation and effects on function. *Exp Eye Res.* 2009; 88:458–466.
10. Jobling AI, Gentle A, Metlapally R, McGowan BJ, McBrien NA. Regulation of scleral cell contraction by transforming growth factor-beta and stress: competing roles in myopic eye growth. *J Biol Chem.* 2009;284:2072–2079.
11. Stone RA, Lin T, Laties AM, Iuvone PM. Retinal dopamine and form-deprivation myopia. *Proc Natl Acad Sci U S A.* 1989;86:704–706.
12. McFadden SA, Howlett MH, Mertz JR. Retinoic acid signals the direction of ocular elongation in the guinea pig eye. *Vision Res.* 2004;44:643–653.
13. Norton TT. Experimental myopia in tree shrews. *Ciba Found Symp.* 1990;155:178–194; discussion 194–179.
14. Rada JA, Shelton S, Norton TT. The sclera and myopia. *Exp Eye Res.* 2006;82:185–200.
15. Gentle A, Liu Y, Martin JE, Conti GL, McBrien NA. Collagen gene expression and the altered accumulation of scleral collagen during the development of high myopia. *J Biol Chem.* 2003;278:16587–16594.
16. McBrien NA, Cornell LM, Gentle A. Structural and ultrastructural changes to the sclera in a mammalian model of high myopia. *Invest Ophthalmol Vis Sci.* 2001;42:2179–2187.
17. Siegwart JT Jr, Norton TT. Steady state mRNA levels in tree shrew sclera with form-deprivation myopia and during recovery. *Invest Ophthalmol Vis Sci.* 2001;42:1153–1159.
18. Ribelayga C, Mangel SC. A circadian clock and light/dark adaptation differentially regulate adenosine in the mammalian retina. *J Neurosci.* 2005;25:215–222.
19. Guggenheim JA, Hill C, Yam TF. Myopia, genetics, and ambient lighting at night in a UK sample. *Br J Ophthalmol.* 2003;87:580–582.
20. Quinn GE, Shin CH, Maguire MG, Stone RA. Myopia and ambient lighting at night. *Nature.* 1999;399:113–114.
21. Smith EL 3rd, Bradley DV, Fernandes A, Hung LF, Boothe RG. Continuous ambient lighting and eye growth in primates. *Invest Ophthalmol Vis Sci.* 2001;42:1146–1152.
22. Norton TT, Amedo AO, Siegwart JT Jr. Darkness causes myopia in visually experienced tree shrews. *Invest Ophthalmol Vis Sci.* 2006;47:4700–4707.
23. Kvanta A, Seregard S, Sejersen S, Kull B, Fredholm BB. Localization of adenosine receptor messenger RNAs in the rat eye. *Exp Eye Res.* 1997;65:595–602.
24. Cui D, Trier K, Chen X, et al. Distribution of adenosine receptors in human sclera fibroblasts. *Mol Vis.* 2008;14:523–529.
25. Che J, Chan ES, Cronstein BN. Adenosine A2A receptor occupancy stimulates collagen expression by hepatic stellate cells via pathways involving protein kinase A, Src, and extracellular signal-regulated kinases 1/2 signaling cascade or p38 mitogen-activated protein kinase signaling pathway. *Mol Pharmacol.* 2007;72:1626–1636.
26. Montesinos MC, Desai A, Chen JF, et al. Adenosine promotes wound healing and mediates angiogenesis in response to tissue injury via occupancy of A(2A) receptors. *Am J Pathol.* 2002;160: 2009–2018.
27. Victor-Vega C, Desai A, Montesinos MC, Cronstein BN. Adenosine A2A receptor agonists promote more rapid wound healing than recombinant human platelet-derived growth factor (Becaplermin gel). *Inflammation.* 2002;26:19–24.
28. Chan ES, Montesinos MC, Fernandez P, et al. Adenosine A(2A) receptors play a role in the pathogenesis of hepatic cirrhosis. *Br J Pharmacol.* 2006;148:1144–1155.
29. Fernandez P, Trzaska S, Wilder T, et al. Pharmacological blockade of A2A receptors prevents dermal fibrosis in a model of elevated tissue adenosine. *Am J Pathol.* 2008;172:1675–1682.
30. Chen JF, Huang Z, Ma J, et al. A(2A) adenosine receptor deficiency attenuates brain injury induced by transient focal ischemia in mice. *J Neurosci.* 1999;19:9192–9200.
31. Yu L, Huang Z, Mariani J, Wang Y, Moskowitz M, Chen JF. Selective inactivation or reconstitution of adenosine A2A receptors in bone marrow cells reveals their significant contribution to the development of ischemic brain injury. *Nat Med.* 2004;10:1081–1087.
32. Bastia E, Xu YH, Scibelli AC, et al. A crucial role for forebrain adenosine A(2A) receptors in amphetamine sensitization. *Neuropsychopharmacology.* 2005;30:891–900.
33. Zhou X, Shen M, Xie J, et al. The development of the refractive status and ocular growth in C57BL/6 mice. *Invest Ophthalmol Vis Sci.* 2008;49:5208–5214.
34. Schaeffel F, Burkhardt E, Howland HC, Williams RW. Measurement of refractive state and deprivation myopia in two strains of mice. *Optom Vis Sci.* 2004;81:99–110.
35. Zhou X, Xie J, Shen M, et al. Biometric measurement of the mouse eye using optical coherence tomography with focal plane advancement. *Vision Res.* 2008;48:1137–1143.
36. Wang J, Aquavella J, Palakuru J, Chung S. Repeated measurements of dynamic tear distribution on the ocular surface after instillation of artificial tears. *Invest Ophthalmol Vis Sci.* 2006;47:3325–3329.
37. Chakravarti S, Petroll WM, Hassell JR, et al. Corneal opacity in lumican-null mice: defects in collagen fibril structure and packing in the posterior stroma. *Invest Ophthalmol Vis Sci.* 2000;41:3365–3373.
38. Ezura Y, Chakravarti S, Oldberg A, Chervoneva I, Birk DE. Differential expression of lumican and fibromodulin regulate collagen fibrillogenesis in developing mouse tendons. *J Cell Biol.* 2000;151: 779–788.
39. Chakravarti S, Paul J, Roberts L, Chervoneva I, Oldberg A, Birk DE. Ocular and scleral alterations in gene-targeted lumican-fibromodulin double-null mice. *Invest Ophthalmol Vis Sci.* 2003;44:2422–2432.
40. Lu F, Zhou X, Xie R, et al. Feasibility of two-dimensional gel electrophoresis used for proteomic analysis of human scleral fibroblasts. *Curr Eye Res.* 2007;32:319–329.
41. Qu J, Zhou X, Xie R, et al. The presence of m1 to m5 receptors in human sclera: evidence of the sclera as a potential site of action for muscarinic receptor antagonists. *Curr Eye Res.* 2006;31:587–597.
42. Schmucker C, Schaeffel F. A paraxial schematic eye model for the growing C57BL/6 mouse. *Vision Res.* 2004;44:1857–1867.
43. Tsai PP, Pachowsky U, Stelzer HD, Hackbarth H. Impact of environmental enrichment in mice. 1: effect of housing conditions on body weight, organ weights and haematology in different strains. *Lab Anim.* 2002;36:411–419.
44. Norton TT, Rada JA. Reduced extracellular matrix in mammalian sclera with induced myopia. *Vision Res.* 1995;35:1271–1281.
45. Birk DE. Type V collagen: heterotypic type I/V collagen interactions in the regulation of fibril assembly. *Micron.* 2001;32:223–237.
46. Schippert R, Burkhardt E, Feldkaemper M, Schaeffel F. Relative axial myopia in Egr-1 (ZENK) knockout mice. *Invest Ophthalmol Vis Sci.* 2007;48:11–17.
47. Pardue MT, Faulkner AE, Fernandes A, et al. High susceptibility to experimental myopia in a mouse model with a retinal on pathway defect. *Invest Ophthalmol Vis Sci.* 2008;49:706–712.
48. Xie R, Zhou XT, Lu F, et al. Correlation between myopia and major biometric parameters of the eye: a retrospective clinical study. *Optom Vis Sci.* 2009;86:E503–E508.
49. Tong L, Wong EH, Chan YH, Balakrishnan V. A multiple regression approach to study optical components of myopia in Singapore school children. *Ophthalmic Physiol Opt.* 2002;22:32–37.
50. McBrien NA, Adams DW. A longitudinal investigation of adult-onset and adult-progression of myopia in an occupational group: refractive and biometric findings. *Invest Ophthalmol Vis Sci.* 1997; 38:321–333.
51. Yang JN, Chen JF, Fredholm BB. Physiological roles of A1 and A2A adenosine receptors in regulating heart rate, body temperature, and locomotion as revealed using knockout mice and caffeine. *Am J Physiol Heart Circ Physiol.* 2009;296:H1141–H1149.
52. Chen JF, Moratalla R, Impagnatiello F, et al. The role of the D(2) dopamine receptor (D(2)R) in A(2A) adenosine receptor (A(2A)R)-mediated behavioral and cellular responses as revealed by A(2A) and D(2) receptor knockout mice. *Proc Natl Acad Sci U S A.* 2001;98:1970–1975.
53. Fredholm BB, Chen JF, Masino SA, Vaugeois JM. Actions of adenosine at its receptors in the CNS: insights from knockouts and drugs. *Annu Rev Pharmacol Toxicol.* 2005;45:385–412.

54. Remtulla S, Hallett PE. A schematic eye for the mouse, and comparisons with the rat. *Vision Res.* 1985;25:21–31.
55. Schmucker C, Schaeffel F. In vivo biometry in the mouse eye with low coherence interferometry. *Vision Res.* 2004;44:2445–2456.
56. Tejedor J, de la Villa P. Refractive changes induced by form deprivation in the mouse eye. *Invest Ophthalmol Vis Sci.* 2003;44:32–36.
57. Barathi VA, Boopathi VG, Yap EP, Beuerman RW. Two models of experimental myopia in the mouse. *Vision Res.* 2008;48:904–916.
58. Fredholm BB, Johansson B, Lindstrom K, Wahlstrom G. Age-dependent changes in adenosine receptors are not modified by life-long intermittent alcohol administration. *Brain Res.* 1998;791:177–185.
59. Schiffmann SN, Vanderhaeghen JJ. Age-related loss of mRNA encoding adenosine A2 receptor in the rat striatum. *Neurosci Lett.* 1993;158:121–124.
60. Lu F, Zhou X, Jiang L, et al. Axial myopia induced by hyperopic defocus in guinea pigs: a detailed assessment on susceptibility and recovery. *Exp Eye Res.* 2009;89:101–108.
61. McBrien NA, Gentle A. Role of the sclera in the development and pathological complications of myopia. *Prog Retin Eye Res.* 2003; 22:307–338.
62. Curtin BJ, Teng CC. Scleral changes in pathological myopia. *Trans Am Acad Ophthalmol Otolaryngol.* 1958;62:777–788; discussion 788–790.
63. Rada JA, Nickla DL, Troilo D. Decreased proteoglycan synthesis associated with form deprivation myopia in mature primate eyes. *Invest Ophthalmol Vis Sci.* 2000;41:2050–2058.
64. Curtin BJ, Iwamoto T, Renaldo DP. Normal and staphylomatous sclera of high myopia: an electron microscopic study. *Arch Ophthalmol.* 1979;97:912–915.
65. Liu KR, Chen MS, Ko LS. Electron microscopic studies of the scleral collagen fiber in excessively high myopia. *Taiwan Yi Xue Hui Za Zhi.* 1986;85:1032–1038.
66. Chan ES, Fernandez P, Merchant AA, et al. Adenosine A2A receptors in diffuse dermal fibrosis: pathogenic role in human dermal fibroblasts and in a murine model of scleroderma. *Arthritis Rheum.* 2006;54:2632–2642.
67. Trier K, Olsen EB, Kobayashi T, Ribel-Madsen SM. Biochemical and ultrastructural changes in rabbit sclera after treatment with 7-methylxanthine, theobromine, acetazolamide, or L-ornithine. *Br J Ophthalmol.* 1999;83:1370–1375.
68. Trier K, Ribel-Madsen SM, Cui DM, Christensen SB. Systemic 7-methylxanthine in retarding axial eye growth and myopia progression: a 36-month pilot study. *J Ocul Biol Dis Inform.* 2008;1:85–93.
69. Fredholm BB, Arslan G, Halldner L, Kull B, Schulte G, Wasserman W. Structure and function of adenosine receptors and their genes. *Naunyn Schmiedebergs Arch Pharmacol.* 2000;362:364–374.
70. Troilo D, Nickla DL, Mertz JR, Summers Rada JA. Change in the synthesis rates of ocular retinoic acid and scleral glycosaminoglycan during experimentally altered eye growth in marmosets. *Invest Ophthalmol Vis Sci.* 2006;47:1768–1777.